
ISVR, Southampton, UK
ACTIVE 2002
2002 July 15-17

HYBRID ISOLATION OF STRUCTURE-BORNE SOUND

C.A.J. Beijers and A. de Boer
University of Twente
P.O. Box 217
7500 AE Enschede
The Netherlands
c.a.j.beijers@wb.utwente.nl

INTRODUCTION

Interior noise problems become more important due to the tendency to construct lighter vehicles. An important source for interior noise in a vehicle is the engine. The structural vibrations induced by the engine will transmit through the vehicle and will finally result in interior noise elsewhere in the vehicle, so-called structure-borne sound. To reduce the interior noise a solution is sought in a combination of passive and active isolation (hybrid isolation) of the engine. A project has been started to investigate this type of isolation and to develop experimentally validated numerical simulations for the design of hybrid isolation system.

This paper focuses on the numerical modelling approach for this type of problems. The model consists of a structural and a bounded acoustic part that are representative for a vehicle. The responses of both parts are determined efficiently with modal superposition. The controller design, necessary for the active part of the isolation, is performed with the optimal control theory that is based on minimization of a cost function. Different cost functions will be compared with each other with emphasis on the performance of the structural related cost functions (e.g. minimization of structural velocities) in comparison with the acoustical cost functions (e.g. minimization of sound pressures).

MODEL DESCRIPTION

In general the motors in vehicles are mounted on passive mounts, e.g. rubbers. These mounts isolate the engine in a certain way from the vehicle. However, because of the tendency for weight reduction (lighter vehicles) and the severe demands of the customers for comfort and stricter government regulations, extra reduction of interior sound is necessary [1,2] by means of a better isolation of the vibration source. A solution is sought in a combination of active and passive isolation of the engine. This paper will focus on the modelling of the active part of hybrid isolation systems [3].

In general some typical components can be distinguished in the considered isolation system as schematically depicted in figure 1(a) [4,5]. First a source is present, representing the engine. Mounts connect the source with the vehicle structure. The latter is also called the receiver structure. The part of the vehicle structure that radiates sound is called the interface. Two cases will be considered concerning the acoustic analysis: sound radiation of the interface into 1) free space and 2) into a rectangular cavity.

For this study a simplified finite element model of a vehicle is used to investigate the performance of active isolation. The receiver consists of a combination of shell and beam elements. The interface is a stiffened plate structure modelled with beam and shell elements such that the model has several dynamic modes in the considered frequency range. The disturbance or primary force $\{F_p\}$ is supposed to act on the top of the mounts by a unit force in the three perpendicular directions. The actuators are defined at the bottom of all the mounts and are modelled by a secondary force acting in the longitudinal direction $\{F_s\}$. The mounts are modelled with beam elements.

Some dimensions of the model are presented in table 1 and the structural material properties in table 2.

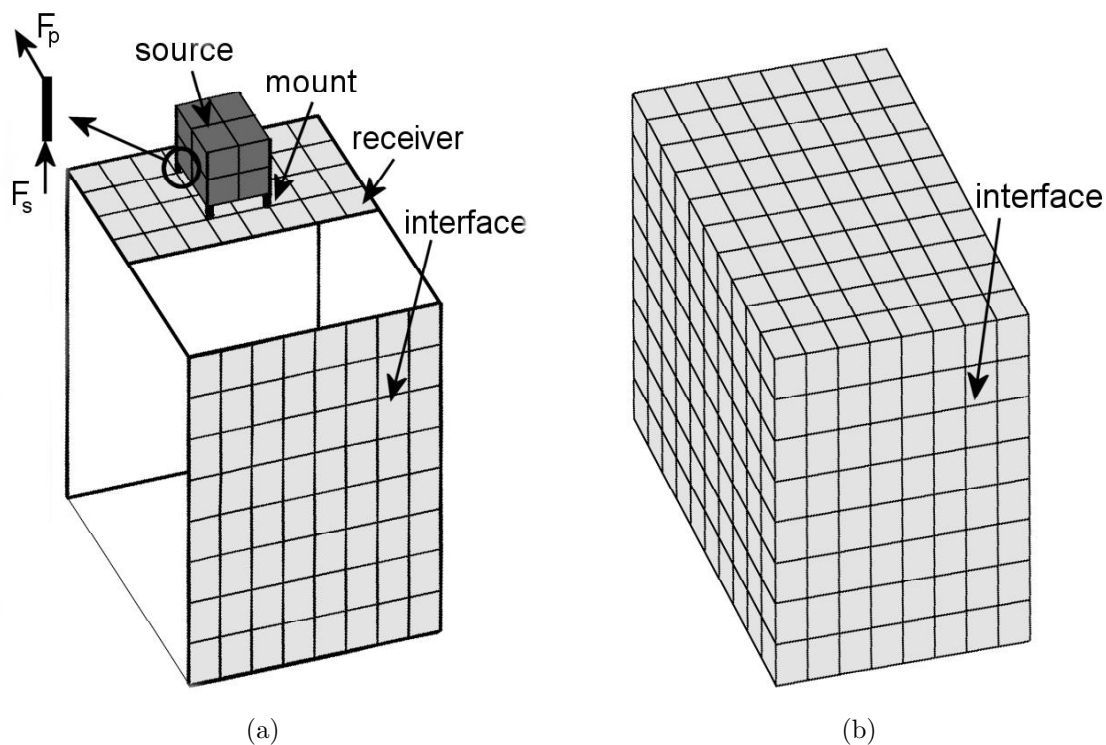


Figure 1: FEM-mesh of the structural part and acoustical part of the model.

	Structure	Cavity
global dimensions	$1 \times 1.5 \times 1.85$ m	$1 \times 1.5 \times 1.85$ m
dimensions interface	1×1.5 m	1×1.5 m
dimensions mounts:	$\text{Ø}60$ mm, $h = 60$ mm	

Table 1: Dimensions of the model

	Material properties structure
elasticity modulus structure	75 GPa
elasticity modulus mount	5 GPa
loss factor	0.02

Table 2: Material properties structure

STRUCTURAL ANALYSIS

The structural response of the total hybrid system is calculated with a reduced model based on modal superposition of the natural modes of the structure. The finite element formulation of the equations of motion of the undamped system with N degrees of freedom is [6]:

$$[M]\{\ddot{u}\} + [K]\{u\} = \{F\} \quad (1)$$

with $[M]$ the $N \times N$ mass matrix, $[K]$ the $N \times N$ stiffness matrix, $[F]$ the $N \times 1$ force vector and $\{u\}$ the vector with the displacements at all N degrees of freedom of the model. The modal representation of this set equation is:

$$\{\ddot{q}\} + [\Omega]^2\{q\} = [\Phi]^T\{F\} \quad (2)$$

With $[\Phi]$ the $N \times m$ modal matrix normalised with respect to the mass matrix $[M]$ (with m the amount of modes: $m \leq N$), $[\Omega]$ the diagonal matrix with m eigenfrequencies and $\{q\}$ the generalized coordinate or modal participation ($\{u\} = [\Psi]\{q\}$). Introducing a modal damping which depends on the eigenfrequency and a constant loss factor η changes equation (3) into:

$$\{\ddot{q}\} + \eta[\Omega]\{\dot{q}\} + [\Omega]^2\{q\} = [\Phi]^T\{F\} \quad (3)$$

For a harmonic analysis the modal participations are determined according to:

$$\{q\} = (-\omega^2[I] + j\omega\eta[\Omega] + [\Omega]^2)^{-1}[\Phi]^T\{F\} \quad (4)$$

With the modal participations the harmonic displacements of all degrees of freedom can be calculated. For structural-acoustic interaction the velocities $\{v\}$ are needed:

$$\{v\} = \{\dot{u}\} = j\omega\{u\} = j\omega[\Phi]\{q\} \quad (5)$$

Considering the hybrid isolation system different structural transfer functions have to be calculated: the transfer functions from the disturbance force (or primary force) $\{F_p\}$ and the actuator force (or secondary force) $\{F_s\}$ to the structural sensors and velocities of the interface plate. The transfer functions from the forces to the velocities at the interface plate are needed to calculate the acoustic response (described in the next section) and to implement active isolation with acoustic sensors (described in the section active isolation).

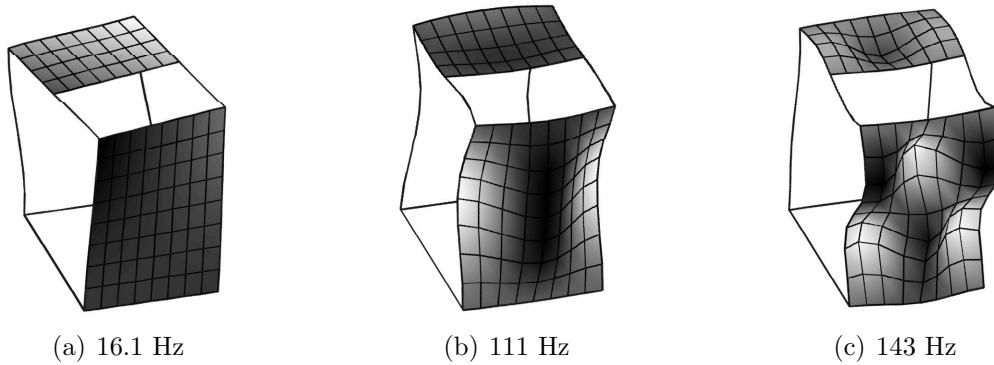


Figure 2: Some structural modes of the receiver with corresponding eigenfrequency

ACOUSTIC ANALYSIS

The vibrations of the structure will result in noise at certain parts of the receiver construction. In this section only the sound radiated by the interface plate will be considered. Two cases will be treated: sound radiation of the interface plate into the free space (exterior problem) and sound radiation into a cavity (interior problem). The cavity can be seen as a simple model of an accommodation in a vehicle.

Sound radiation into free space

A few assumptions are made to model the free field radiation. The calculation of the sound power is uncoupled: the sound pressures have no influence on the structural vibrations. The interface plate is flat and is considered to be situated in a baffle (an infinite large rigid plate) [7,8].

With these assumptions the general Kirchhoff-Helmholtz equation that describes the sound pressure p at location \mathbf{r} in the free field can be written as [9]:

$$p(\mathbf{r}) = \int_S \frac{j\omega\rho v(\mathbf{r}_s)e^{-jkR}}{2\pi R} dS \quad (6)$$

with ρ the density of air, $v(\mathbf{r}_s)$ the velocity at the location \mathbf{r}_s on the surface S , k the wave number in air ($k = \frac{\omega}{c}$), c the speed of sound in air and R the distance between the

field point and the source location on the surface: $R = |(\mathbf{r} - \mathbf{r}_s)|$. The radiated sound power is taken as measure for the amount of noise generated by the interface plate. To calculate the radiated sound power the pressure distribution on the interface plate has to be calculated. The pressure at one surface point can be calculated according to:

$$\tilde{p}(\mathbf{r}_s) = j\omega\rho \sum_{i=1}^{nelem} \int_{S_e} \frac{e^{-jkR}}{2\pi R} N(x, y) dS_e \{ \tilde{v}(\mathbf{r}_s) \} \quad (7)$$

where $\tilde{\cdot}$ denotes the value at the nodal points, $\tilde{p}(\mathbf{r}_s)$ the pressure at a nodal point on the surface of the interface, $nelem$ the amount of elements on the surface, $N(x, y)$ the shape functions (for linear quadrilateral elements) in the in plane coordinates x and y of the interface plate, S_e the area of the element and $\{ \tilde{v}(\mathbf{r}_s) \}$ a vector with the normal velocities at all nodes on the surface. The integration over the element itself is performed numerically with Gauss quadrature [10]. When the pressure is calculated at each nodal point on the surface the impedance matrix $[Z]$ can be composed:

$$\{p(\mathbf{r}_s)\} = [Z]\{v(\mathbf{r}_s)\} \quad (8)$$

The radiated sound power W is calculated by:

$$W = \frac{1}{2} \text{Re} \int_S v^*(\mathbf{r}_s) p(\mathbf{r}_s) dS \quad (9)$$

where $*$ denotes the complex conjugate.

$$W = \frac{1}{2} \text{Re} \{ \{v(\mathbf{r}_s)\}^H \sum_{i=1}^{nelem} \int_{S_e} N^H(x, y) N(x, y) dS_e \{p(\mathbf{r}_s)\} \} \quad (10)$$

where H denotes the hermitian transposed. When equation 10 is evaluated a matrix B can be composed. Together with equation (8) the radiated power can finally be calculated by:

$$W = \frac{1}{2} \text{Re} \{ \{v(\mathbf{r}_s)\}^H [B] [Z] \{v(\mathbf{r}_s)\} \} \quad (11)$$

Sound in rectangular cavity

In cavities the air is bounded by walls and the pressure distribution can be described by a superposition of the eigenmodes of the cavity [9]. The eigenmodes are calculated by the Finite Element package ANSYS with the mesh as plotted in figure 1(b). The cavity is assumed to have rigid walls, except at the interface and the calculation is performed uncoupled (no influence of the pressure on the structural motion). The response of the cavity will be determined by a modal superposition of the modes of the rigid cavity. The modes are calculated with the finite element package ANSYS. The measure for the amount of noise in the cavity is determined by the sound pressure distribution in the cavity. The equation for the pressure in the cavity in terms of the Green's function $G(\mathbf{r}|\mathbf{r}_s)$ is:

$$\{p(\mathbf{r})\} = j\omega\rho \sum_{i=1}^{nelem} v_i S_i G(\mathbf{r}|\mathbf{r}_s) \quad (12)$$

with v_i the normal velocity associated with an element on the interface, S_i the area of the element and $nelem$ the amount of elements on the interface. The Green's function can be expressed by a summation over the eigenmodes of the cavity according to:

$$G(\mathbf{r}|\mathbf{r}_s) = \sum_{j=1}^{nmode} A_j \{\Psi_j(\mathbf{r})\} \quad (13)$$

with $nmode$ the amount of modes taken into account, A_j the participation factor for mode j and $\Psi_j(\mathbf{r})$ the acoustic mode j of the cavity (see figure 3). When equation (13)

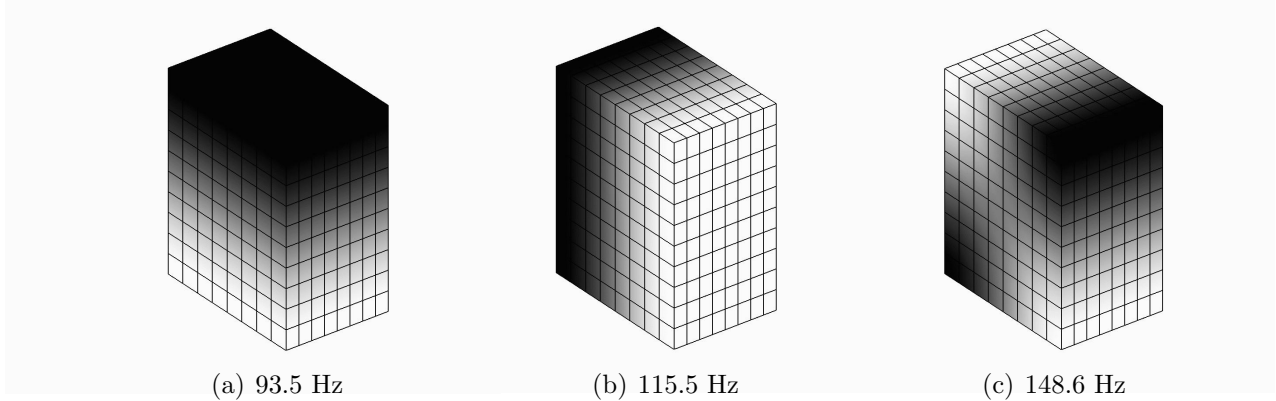


Figure 3: The pressure distribution of the 2nd, 3rd and 4th acoustic mode of the cavity

is used to solve the general Helmholtz equation and making use of the fact that the eigenmodes of the cavity satisfy the homogeneous Helmholtz equation yields the following expression for the Green's function:

$$G(\mathbf{r}|\mathbf{r}_s) = \sum_{j=1}^{nmode} \frac{\Psi_j(\mathbf{r}_s)}{\Lambda_j(k_j^2 - k^2)} \{\Psi_j(\mathbf{r})\} \quad (14)$$

with k_j the j^{th} eigenvalue of the cavity and Λ_j the modal volume of the j^{th} eigenmode:

$$\Lambda_j = \int_V \Psi_j(\mathbf{r})^2 dV \quad (15)$$

The modes shape vectors can be normalized to the mass matrix:

$$\hat{\Psi}_j^T [M] \hat{\Psi}_j = 1 \quad (16)$$

or the largest factor can be normalized to unity:

$$\tilde{\Psi}_j^T [M] \tilde{\Psi}_j = \frac{\Lambda_j}{c^2} \quad (17)$$

Now the following relationship for the modal volume can be derived for $\tilde{\Psi}_j$ [11]:

$$\Lambda_j = \frac{c^2}{\max(\hat{\Psi}_j)^2} \quad (18)$$

When equation (12) is evaluated for (a part of) the nodal pressure points in the cavity, an impedance matrix $[Z_{cav}]$ can be composed. This impedance matrix relates the considered pressures in the cavity (placed in the vector $\{p(\mathbf{r})\}$) to the nodal normal velocities at the interface according to:

$$\{p(\mathbf{r})\} = [Z_{cav}]\{v(\mathbf{r}_s)\} \quad (19)$$

A good measure for the amount of noise in the cavity is the sum of the squared pressures: $\{p\}^H\{p\}$.

ACTIVE ISOLATION

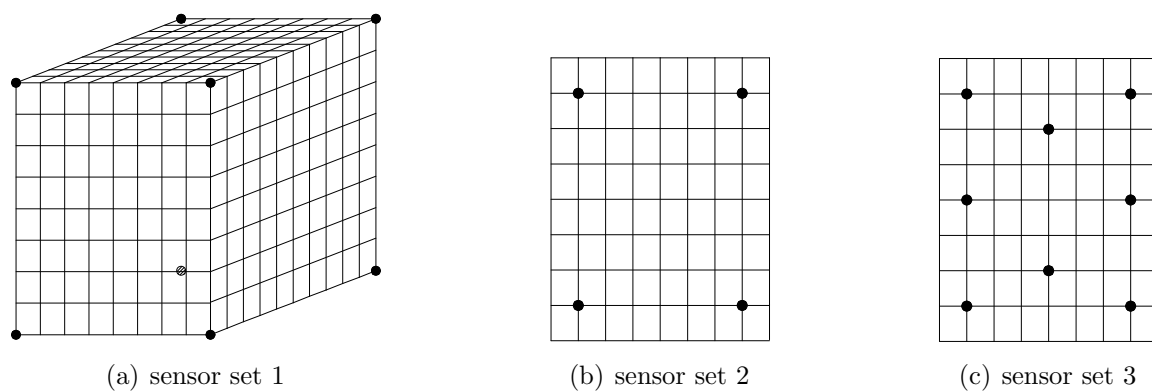


Figure 4: The different sensor sets used in the simulations

In the preceding section the calculation of different transfer functions is explained. It is assumed that the excitation of the source is harmonic with the rotational speed of the motor. This is known information which can be used as reference signal for the controller, so a feedforward control strategy [12] can be used to reduce the response. The calculation of the actuator forces and active response in the numerical example is determined with the optimal control theory [13]. The optimal actuator force is calculated by minimization of a quadratic cost function such as:

- minimization of velocities at discrete locations on the structure
- minimization of pressures at discrete locations in the cavity
- minimization of radiated sound power

The quantity to be minimized is in practice a sensor that measures the response at the specified locations.

The total response at the sensor positions can in general be written in hermitian quadratic form according to:

$$J = ([H_p]\{F_p\} + [H_s]\{F_s\})^H ([H_p]\{F_p\} + [H_s]\{F_s\}) \quad (20)$$

with J the response in quadratic form of the sensors, H_p the transfer from the disturbance forces to the sensors and H_s the transfer from the actuator forces to the sensors. The optimal set of actuator forces that minimizes the cost function and in fact minimizes the response at the sensor locations is:

$$\{F_{s,opt}\} = -[A]^{-1}\{b\} \quad (21)$$

with $\{F_{s,opt}\}$ the vector with optimal actuator forces and

$$[A] = [H_s]^H [H_s] \quad (22)$$

$$\{b\} = [H_s]^H [H_p] \{F_p\} \quad (23)$$

Consider for example the cost function $p^H p$. When the structural transfer function from the force to velocity of the interface plate is defined as $[Hv]$ and making use of equation (19) the response described by the cost function is:

$$\{p\}^H \{p\} = ([Z_{cav}][Hv_p]\{F_p\} + [Z_{cav}][Hv_s]\{F_s\})^H ([Z_{cav}][Hv_p]\{F_p\} + [Z_{cav}][Hv_s]\{F_s\}) \quad (24)$$

The optimal actuator force that minimizes the cost function $p^H p$ is:

$$\{F_{s,opt}\} = -([Hv_s]^H [Z_{cav}]^H [Z_{cav}][Hv_s])^{-1} ([Hv_s]^H [Z_{cav}]^H [Z_{cav}][Hv_p]\{F_p\}) \quad (25)$$

As a next step the active response can be calculated with equation (24) with substitution of the determined optimal actuator forces $\{F_{s,opt}\}$ for $\{F_s\}$. In the figures 4(a), 4(b) and 4(c) the considered sensor sets are depicted as used in the simulations.

Sensor set 1 is a set of eight microphones placed in the corners of the cavity, sensor set 2 and 3 are velocity sensors at different locations on the interface plate of the structure.

RESULTS

In this section some results of the active isolation will be presented. First the influence of minimization of the velocities (sensor set 2 and 3) on the radiated sound power into the free space is calculated. As can be seen in figure 5 a reduction of the radiated sound power can be achieved in most frequency regions. Sensor set 3 results in more reduction of the radiated power as sensor set 2 because this set is more capable to describe the velocity field of the interface plate. At relatively high frequencies the achieved reduction will become less, because of the increasing modal overlap of the structure and the complex dynamic deformations of the structure. Instead of reduction the radiated sound power even increases.

In figure 6 the results for the pressure distribution in the cavity are plotted for sensor set 1. First it can be seen that a lot more eigenfrequencies are present in comparison with the radiated sound power response. This is the consequence of the cavity which has a lot of eigenfrequencies in the considered frequency range. It can also be seen that a very good reduction can be achieved with only 8 microphones in the corners of the cavity. The cavity has rigid walls, so the pressure response will be maximum at the walls. The

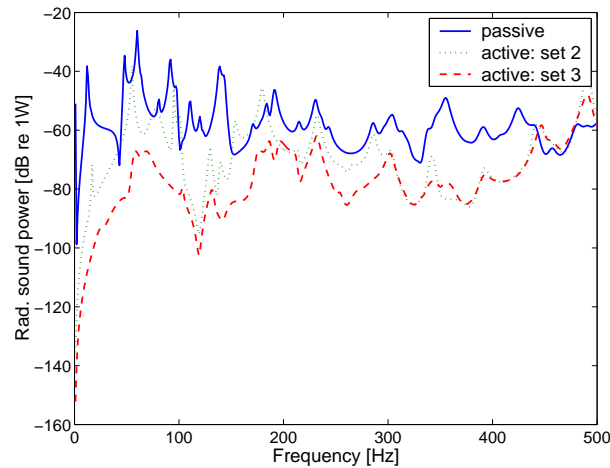


Figure 5: Active response with velocity sensors

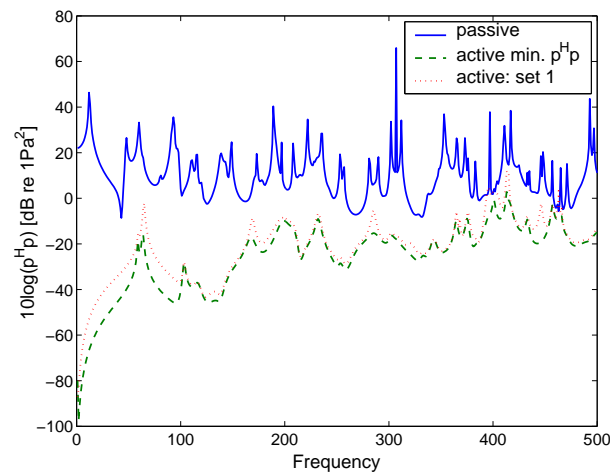


Figure 6: Active response with pressure sensors (sensor set 1)

sensors will consequently have a good signal over the whole frequency range. The line which shows the largest reduction is the active response when the quadratic pressure is minimized for all pressure points. This line represents the most achievable reduction for this model. Instead of pressure sensors, also structural sensors can be used. In figure 7 the active response of the pressure distribution in the cavity is plotted for sensor set 2 and 3. A reduction can be achieved in some frequency ranges. Again the amount of sensors is important for the achievable reduction. Sensor set 3 results in a larger reduction than sensor set 2 especially at the lower frequency region (1 till 300 Hz.). In the higher frequency region (above about 400 Hz.) no reduction is achieved. Also can be seen that at some frequencies where the response is dominated by the cavity response (at eigenfrequencies of the cavity) no reduction can be achieved. The velocity sensors on the interface of the structure cannot 'measure' the increasing pressure response of the cavity in this model, in contrary to the results achieved by sensor set 1. The active response with sensor set 1 (see figure 6) shows no large peaks at the frequencies corresponding to the eigenfrequencies of the cavity.

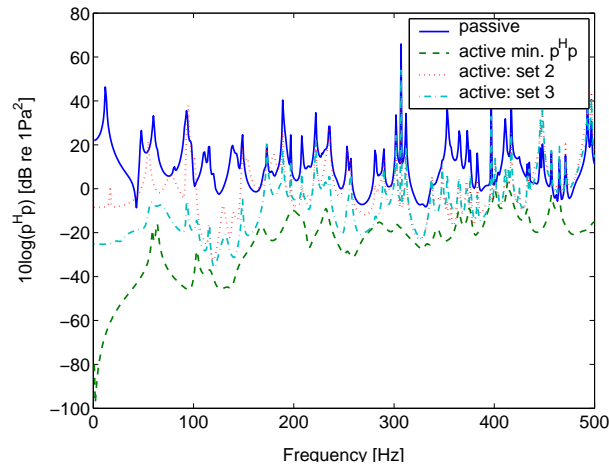


Figure 7: Active response with structural sensors (sensor set 2 and 3)

Except the achievable reduction it is also important to consider the actuator force. The development of actuators is a hot issue, but the magnitude of the forces that can be reached is (very) limited. In Figure 8 a typical plot of the actuator force as function of the frequency is shown for an active isolation system. At low frequencies very large actuator forces are needed to achieve considerable reduction. At these frequencies the receiver has so-called global modes with large deformations. To counteract these relatively large deformations large actuator forces are needed.

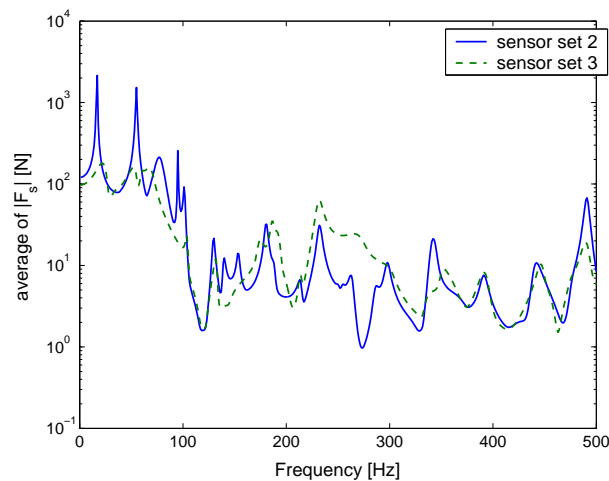


Figure 8: The average value of actuator force for sensor set 2 and 3

DISCUSSION

A hybrid isolation system is presented with acoustic interaction. As can be seen generally large reductions can be achieved with active isolation, but at low frequency

regions large actuator forces are needed. In practice the achieved reductions will not be reached. This is a consequence of the influence of the controller that in fact performs a real time minimization of a cost function, noise of sensor signals, external disturbances, limited actuator forces etc. The goal of the models is not to describe exactly the response of such complex systems, but to get an impression of the tendencies.

The presented modelling method forms a good base for further analysis of isolation systems. It is possible to analyze the influence of e.g. actuator and sensor locations. Except the considered cost functions, also other cost functions can be analyzed, for example reactive or active acoustic power into cavity, combination of different types of sensors, weighting of actuator forces in the cost functions etc. Further experimental verifications will be carried out with a structure like the considered numerical model.

ACKNOWLEDGEMENTS

This research was carried out under the joint research program "Hybrid Isolation of Structure Borne Sound" from TNO Institute of Applied Physics and the University of Twente.

REFERENCES

1. T.L. Lagö, M. Winberg, and S. Johansson. AVIIS, Active Vibration Isolation in Ships: Source identification and ANVC approach. *Fifth International Congress on Sound and Vibration*, pages 477–484, 1997.
2. M. Winberg, S. Johansson, and I. Claesson. AVIIS, Active Vibration Isolation in Ships; an ASAC approach. *Active 1999 Proceedings*, pages 199–207, 1999.
3. C.R. Fuller, S.J. Elliott, and P.A. Nelson. *Active Control of Vibration*. Academic Press, London, 1997.
4. P. Gardonio, S.J. Elliott, and R.J. Pinnington. Active isolation of structural vibration on a multiple-degree-of-freedom system, part i: The dynamics of the system. *Journal of Sound and Vibration*, 207(1):61–94, 1997.
5. P. Gardonio, S.J. Elliott, and R.J. Pinnington. Active isolation of structural vibration on a multiple-degree-of-freedom system, part ii: Effectiveness of active control strategies. *Journal of Sound and Vibration*, 207(1):95–122, 1997.
6. L. Meirovitch. *Elements of Vibration Analysis*. McGraw-Hill, New York, 1986.
7. S.J. Elliott and M.E. Johnson. Radiation modes and the active control of sound power. *Journal of the Acoustical Society of America*, 94(4):2194–2204, 1993.

8. M. N. Currey and K. A. Cunefare. The radiation modes of baffled finite plates. *Journal of the Acoustical Society of America*, 98(3):1570–1580, 1995.
9. F. Fahy. *Foundations of Engineering Acoustics*. Academic Press, London, 2001.
10. R.D. Ciskowski and C.A. Brebbia. *Boundary Element Methods in Acoustics*. Computational Mechanics Publications, Southampton, 1991.
11. B.S. Cazzolato. *Sensing systems for Active Control of Sound into Cavities*. The University of Adelaide, Adelaide, 1999.
12. S.M. Kuo and D.R. Morgan. *Active Noise Control System: Algorithms and DSP Implementations*. John Wiley & Sons, New York, 1996.
13. P.A. Nelson and S.J. Elliott. *Active Control of Sound*. Academic Press, London, 1992.